Electronic Supplement Materials

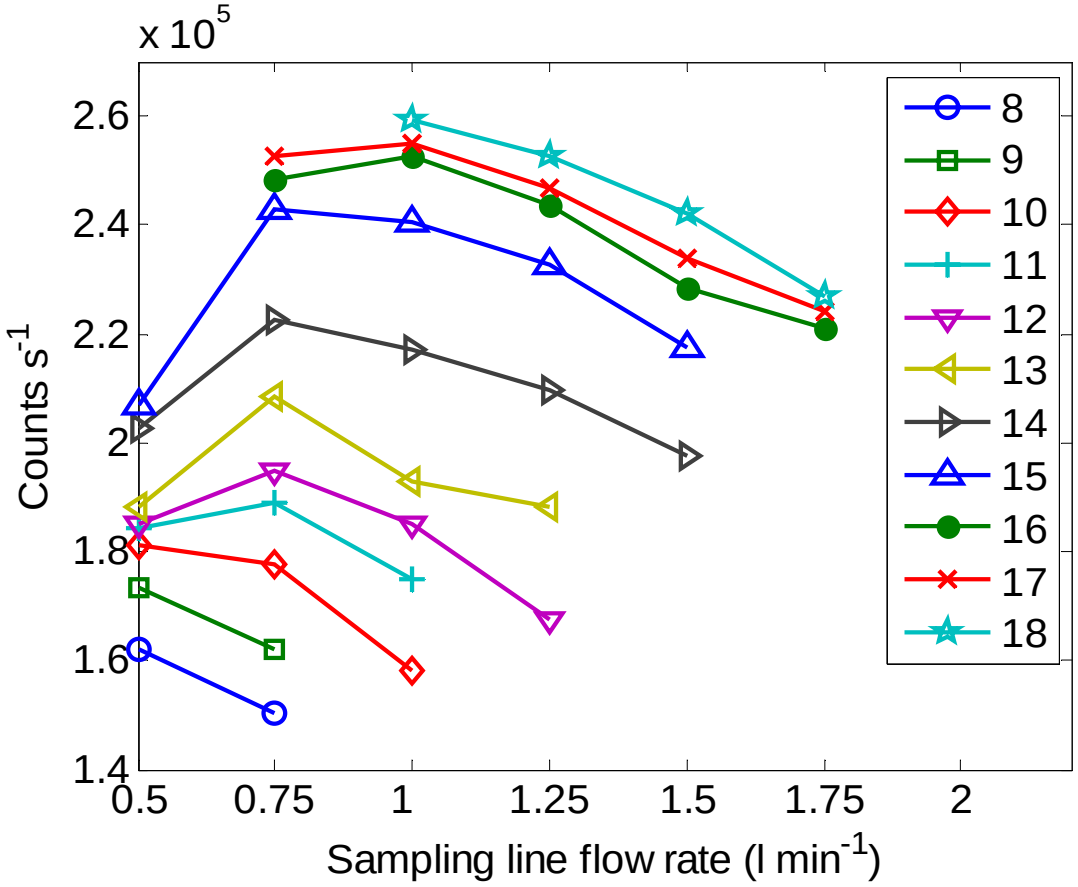

Figure S-1. Instrument response (in counts s^{-1}) as a function of sample flow rate (l min^{-1} through the reaction chamber, and for different reaction chamber pressures (in Torr).

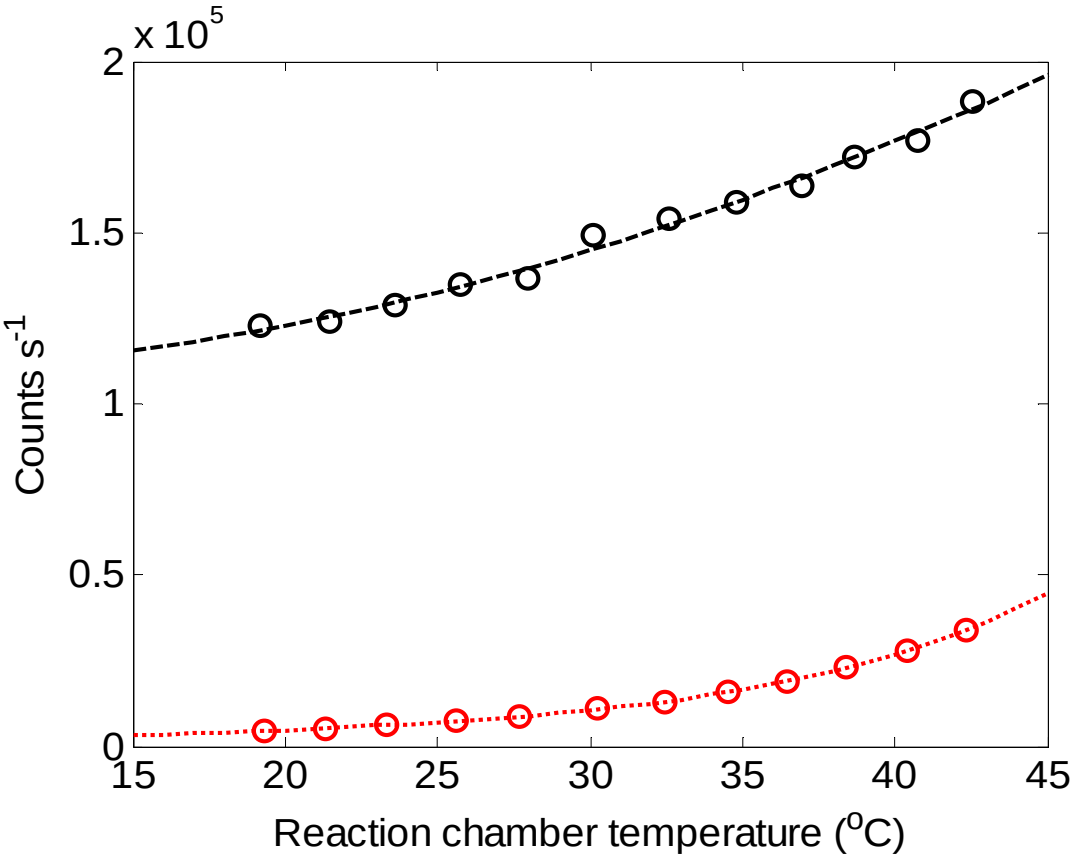

Figure S-2. Instrument response (in counts s^{-1}) as a function of reaction chamber temperature (°C) for a constant O_3 concentration. Black circles show the total signal and the red circles show the background signal at zero ozone concentration. The increase in the background signal at higher temperatures is associated with the warming of the PMT from heat transfer from the reaction chamber, which leads to more thermo-ionic emission.

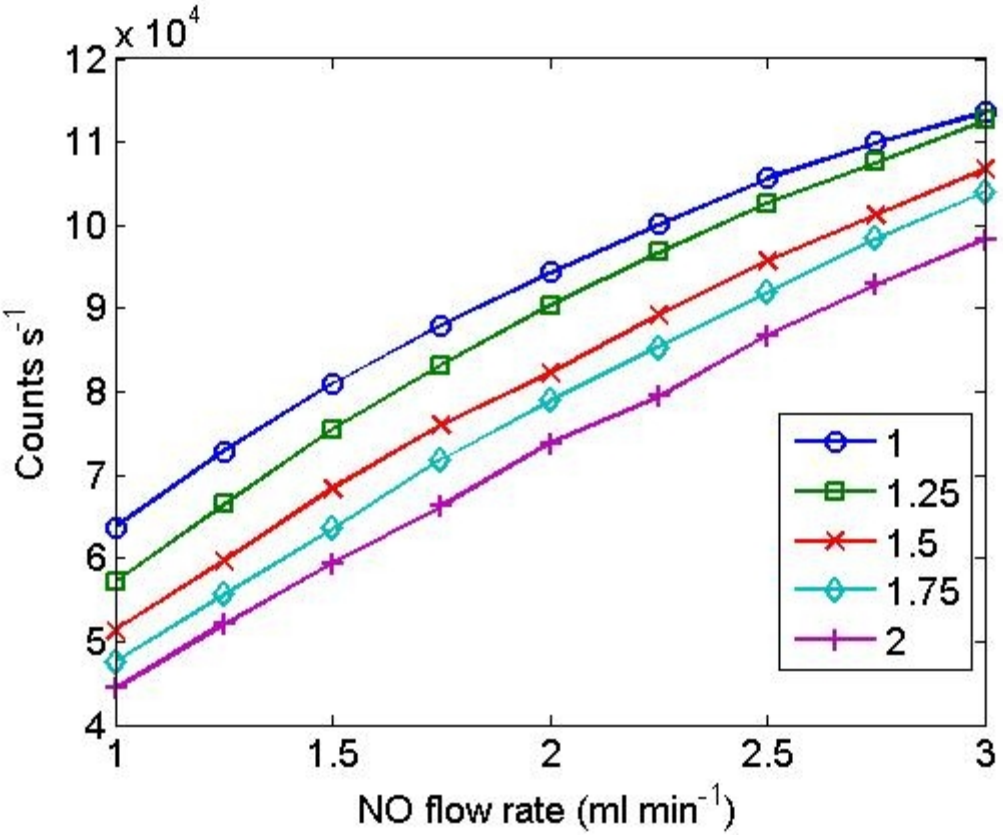

Figure S-3. Instrument response (in counts s^{-1}) as a function of nitric oxide flow rate (ml min^{-1}), and for different sample flow rates into the reaction chamber (l min^{-1}).

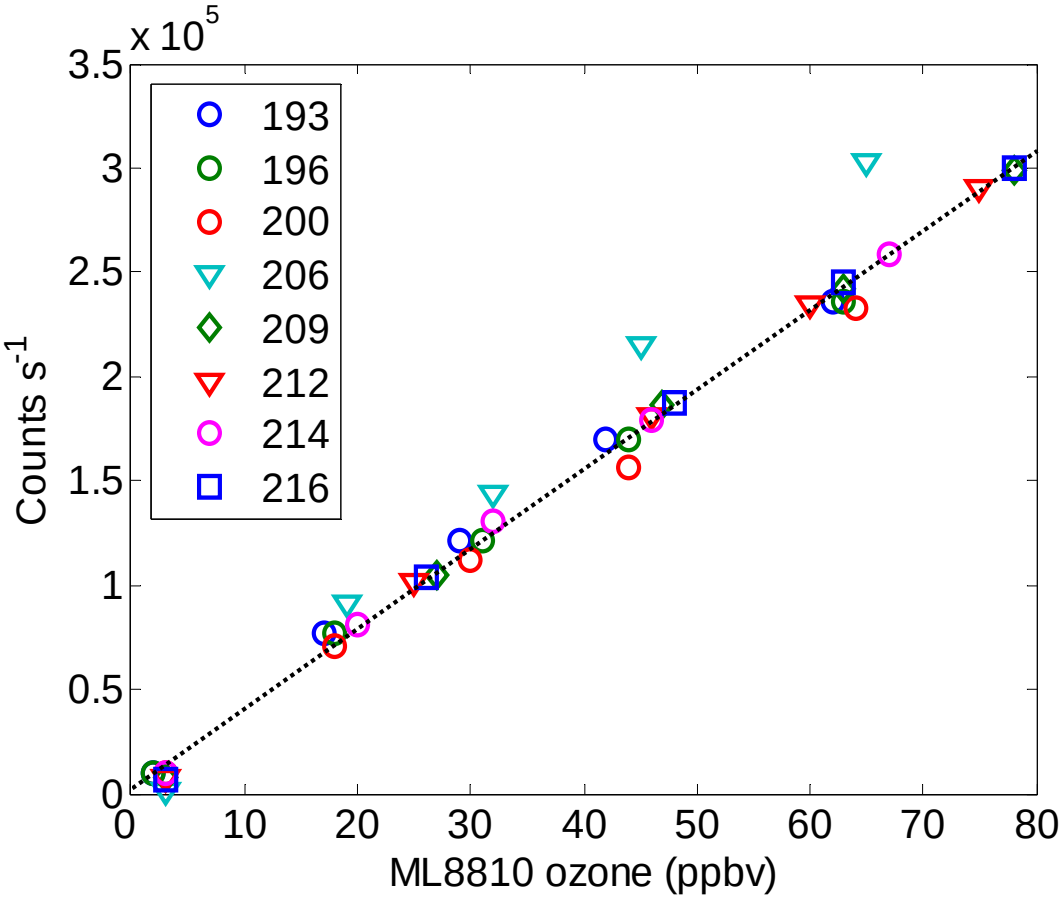

Figure S-4. Calibration of the fast response ozone chemiluminescence instrument (FRCI) with the Monitor Lab (ML) 8810 during the GOMECC-2007 cruise (Day of Year calibrations as indicated in the figure legend).

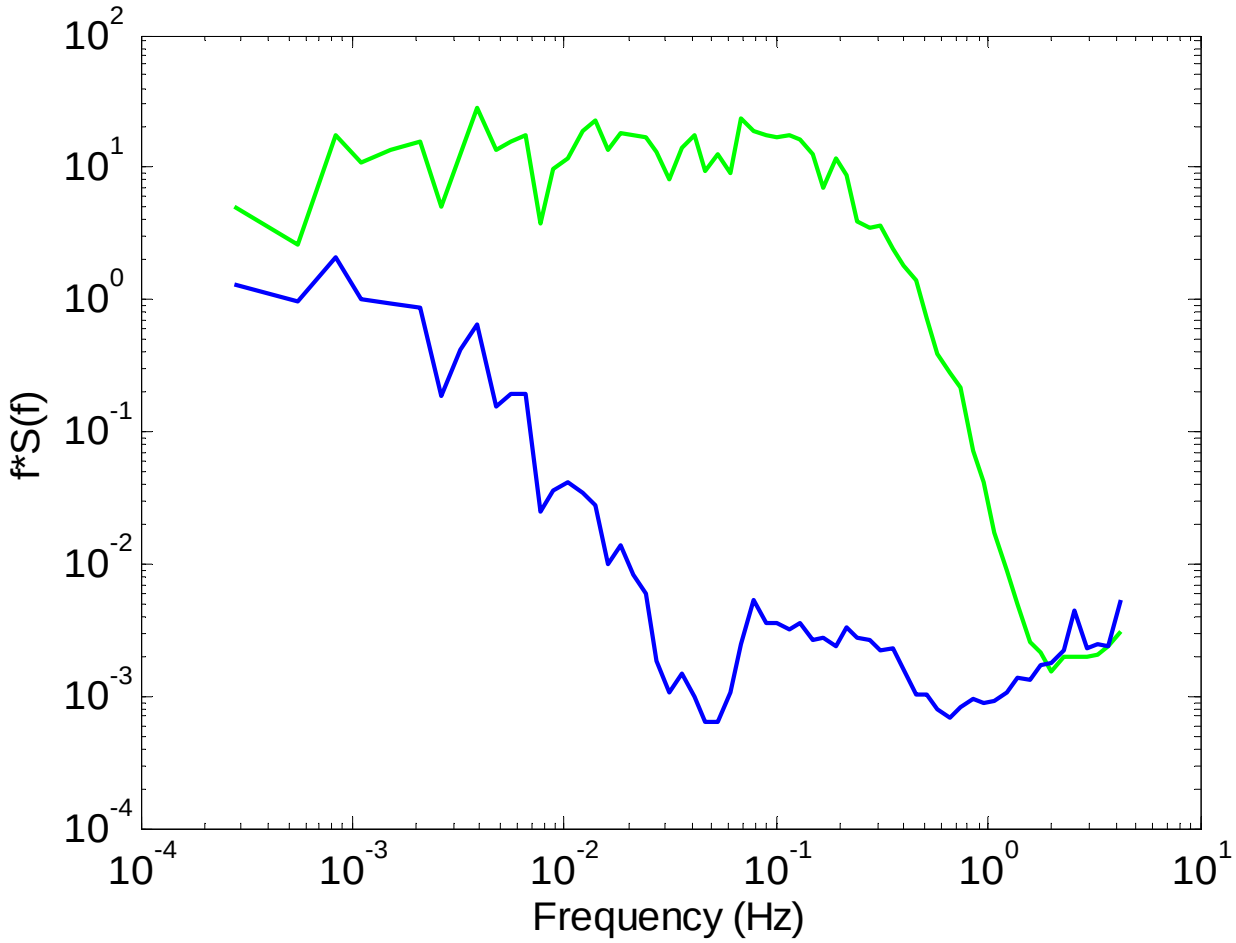

Figure S-5. Power spectrum of the water vapour flux measured with the LI-COR upstream of the Nafion Dryer (green data points) in comparison to the measurements from the LI-COR downstream of the Navion Dryer (blue data).

Signal to Noise Ratio Considerations

In this section we consider the two principal sources of noise which contribute to the S/N ratio. One source is the dark current noise from the PMT detector, and the second one is the shot noise or statistical noise. The total number of counts measured by the FRCI can be expressed as:

$$N_t = (\xi \times X \times \Delta t) + (N_{DC} \times \Delta t) \qquad \text{(Eq. S-1)}$$

where N_t is the total number of counts measured in Δt, ξ is the sensitivity of the instrument (in counts s^{-1} $ppbv^{-1}$ of ozone), Δt is the measurement time (in sec), X is the ozone mixing ratio (in ppbv) and N_{DC} is the number of counts per sec resulting from the dark current.

From the point of view of counting statistics, the S/N ratio can be estimated by the number of counts divided by the square root of the number of counts. Unwanted background counts (dark current) must be subtracted from the measured background plus signal count. Thus, the S/N ratio can be expressed as:

$$\frac{S}{N} = \frac{\xi \times \Delta t \times X}{\sqrt{\xi \times X \times \Delta t + N_{DC} \times \Delta t}} = \sqrt{\frac{\xi \times \Delta t \times X}{1 + \frac{N_{DC}}{\xi \times X}}} \qquad \text{(Eq. S-2)}$$

If the background rate N_{dc} is small or inexistent with respect to the signal count rate ($\xi \times X$), the S/N ratio reduces to $\sqrt{\xi \times X \times \Delta t}$, the square root of the total signal counts. From this equation, it follows that at lower ozone levels, the dark current will have a bigger effect on the S/N ratio than at higher ozone concentration. For instance, with a dark current value of 3500 cts s^{-1} and an ozone concentration of 2 ppbv, the dark current will have a ~30% effect on the S/N ratio. On the other hand, it will only be a 3% effect for a 20 ppbv ozone level.

Other additive sources of noise will contribute to a reduction in the S/N ratio, for example noise from the various electronic circuits used in the instrument. Figure S-6 shows results from two sets of experiments investigating the experimental S/N ratio in comparison to the theoretical value. The theoretical S/N was calculated according to Eq. S-2. The experimental S was taken as the man of counts over a 1-min measurement period, and S was derived as the standard deviation of the 10 Hz data over that same period. The blue data resulted from a calibration experiment, where ozone standards from an ozone generator source were sampled with the instrument. For this experiment, the theoretical S/N at all sampled ozone mixing ratios is 1.17 ± 0.01 larger than the experimentally determined one, indicating a ~15% deterioration of the theoretical S/N from other (than counting statistics and dark current) contributing sources of measurement noise. The other experiment shown resulted from ambient air flux measurements using the FRCI (in this case operated with a 2% NO mixture (in N_2) and a resulting sensitivity of ~2200 counts s^{-1} $ppbv^{-1}$) over snow. Here, the ratio of the theoretical S/N ratio over the experimentally determined value is 1.28 ± 0.28. Under

these conditions the calculated 'noise' in the ambient ozone measurement results from instrument noise as well as from fluctuations in the ozone mixing ratio, i.e. contributions from the ozone flux ($w'O_3'$). Therefore the difference between the experimentally determined and the theoretical S/N ratio is, as expected, larger, than during the sampling of the ozone standard, with the variability of [O_3] from the flux (i.e. O_3') contributing ~ 1/3 of the decrease of the S/N in comparison to the theoretical value.

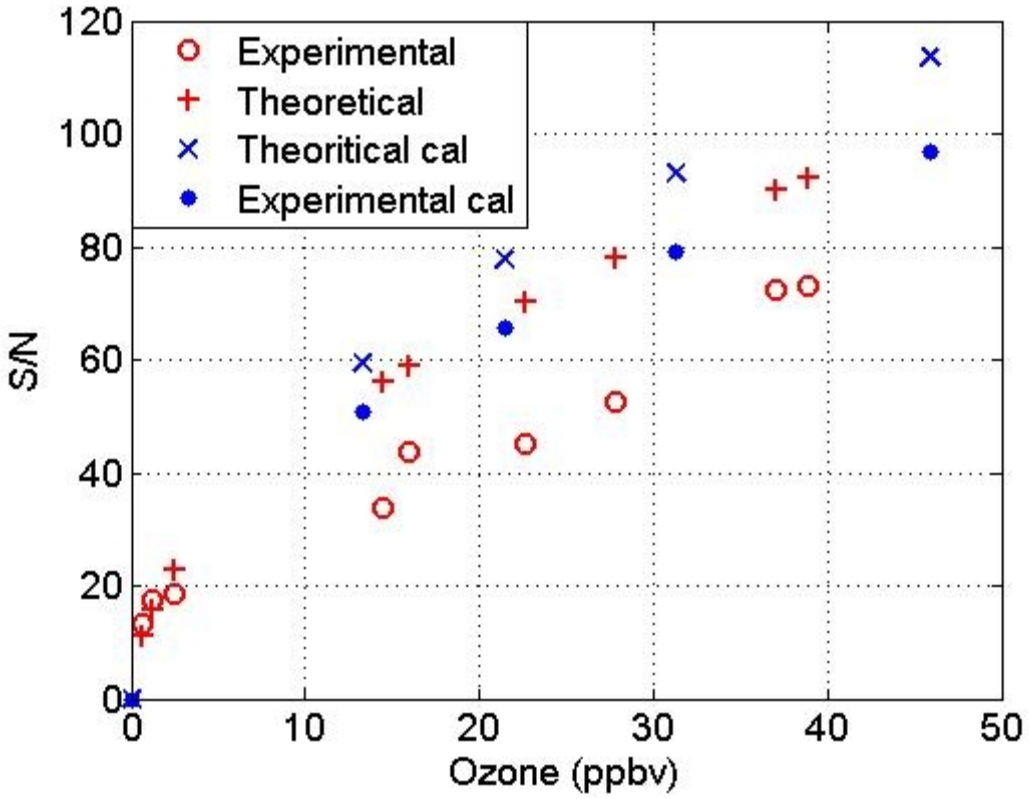

Figure S-6

S/N ratio obtained with the FRCI. Two different sets of experiments are displayed. The blue data resulted from a calibration experiment, where ozone standards from an ozone

generator were sampled. The red data were obtained during ambient flux measurements (in this case over snow-covered, frozen ground in Barrow, Alaska) where the instrument was operated with a 2% NO mixture (in N_2) and with a sensitivity of ~2200 counts s^{-1} $ppbv^{-1}$ (blue circles). Data reflect results from 1-min intervals at different ambient ozone levels. Theoretical values result from the counting statistic expression (Eq. S-2).